THE JOURNAL OF PHYSICAL CHEMISTRY B
A JOURNAL OF THE AMERICAN CHEMICAL SOCIETY

pubs.acs.org/JPCB

Article

Near-Infrared Fluorescent Probes with Rotatable Polyacetylene Chains for the Detection of Amyloid-β Plaques

Longfei Zhang, Xin Gong, Chuan Tian, Hualong Fu,* Hongwei Tan, Jiapei Dai, and Mengchao Cui*

Cite This: *J. Phys. Chem. B* 2021, 125, 497−506

Read Online

ACCESS | Metrics & More | Article Recommendations | Supporting Information

ABSTRACT: The plaques of accumulated β-amyloid (Aβ) in the parenchymal brain are accepted as an important biomarker for the early diagnosis of Alzheimer's disease (AD). Many near-infrared (NIR) probes, which were based on the D−π−A structure and bridged by conjugated double bonds, had been reported and displayed a high affinity to Aβ plaques. Considering the isomerization caused by the polyethylene chain, however, the conjugated polyacetylene chain is a better choice for developing new NIR Aβ probes. Hence, in this report, a new series of NIR probes with naphthyl or phenyl rings and different numbers of conjugated triple bonds were designed, synthesized, and evaluated as NIR probes for Aβ plaques. Upon interaction with Aβ aggregates, these probes displayed a significant increase in fluorescence intensity (45- to 360-fold) and a high to moderate affinity (6.05−56.62 nM). Among them, probe **22b** displayed excellent fluorescent properties with a 183-fold increase in fluorescence intensity and an emission maximum at 650 nm after incubated with Aβ aggregates. Furthermore, **22b** had a high affinity to Aβ aggregates (K_d = 12.96 nM) and could efficiently detect the Aβ plaques in brain sections from both transgenic mice and AD patients *in vitro*. In summary, this work may lead to a new direction in the development of novel NIR probes for the detection of Aβ plaques.

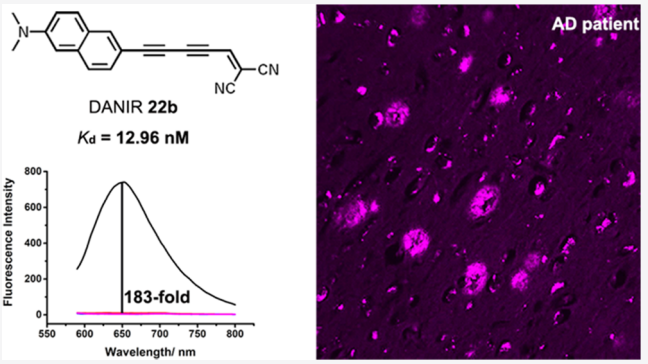

1. INTRODUCTION

Alzheimer's disease (AD) was significantly associated with aging.[1] It could cause dementia, logagnosia, disorientation, and lapsus memoriae, which would bring a heavy burden to the patient's family and the whole society.[2−4] According to the Aβ cascade hypothesis, deposition of amyloid plaques that consist of aggregated Aβ peptides is the hallmark of AD.[5−9] Development of probes targeting to Aβ plaque is essential for monitoring AD's condition, distinguish other types of dementia, and help to test drug efficacy in pharmaceutical development.

In *in vivo* biological imaging, optical imaging technology using the near-infrared (NIR) spectroscopy band (650−900 nm) has many advantages including real-time imaging and sufficient light penetration depth in biological tissues.[6,10,11] Thus, NIR imaging has received increasing attention in recent years, and the research of the NIR fluorescent probe is an important part of this.[12−16] In recent years, a variety of NIR fluorescent probes for Aβ plaques have been reported by our group, including DANIR **2c** and **3c** (Figure 1A).[11,17] In 2014, DANIR **2c**, in which the electron donor (D) and acceptor (A) moieties were bridged by three conjugated C═C bonds, was reported to have a moderate affinity to Aβ aggregates (K_d = 26.9 nM) and has been successfully used in *in vivo* NIR imaging.[11] In 2015, further modification of DANIR **2c** led to the development of DANIR **3c** by replacing the benzene ring with a naphthalene ring.[17] DANIR **3c** was demonstrated to be an excellent *in vivo* NIR probe for Aβ

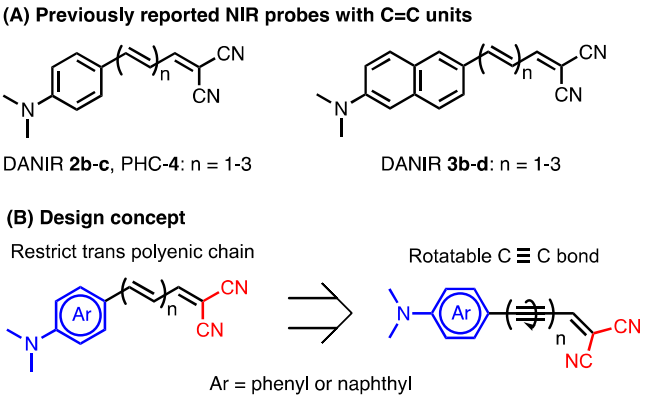

Figure 1. (A) Chemical structures of previously reported Aβ NIR probes with polyene chain. (B) The design concept of our new D−π−A probes with rotatable polyacetylene chain.

Received: September 29, 2020
Revised: December 16, 2020
Published: January 8, 2021

Table 1. Spectroscopic and Binding Data for the Synthesized Probes

probe	λ_{em1}[a] (nm)	λ_{em2}[a] (nm)	Φ_{fl}[b] (%)	fold[c]	K_d[d] (nM)	clog P[e]	E[f] (kcal/mol)
21a	580	535	0.2/0.2	360	18.74 ± 4.86	2.60	6.28
21b	576	602	0.3/0.6	167	6.05 ± 2.02	2.91	3.77
21c	649	649	0.3/0.3	80	51.54 ± 3.2	3.30	1.88
22a	627	603	0.4/1.8	263	12.19 ± 1.36	3.72	5.02
22b	520	650	0.3/0.2	183	12.96 ± 3.19	3.80	2.51
22c	596	665	0.4/0.5	45	56.62 ± 11.11	4.27	6.28
DANIR **2c**[11]	660	659	4.1/0.2	12	26.9 ± 3.0	2.95	18.20
DANIR **3c**[17]	720	678	9.0/0.009	280	1.9 ± 1.1	4.05	16.94

[a]Emission maxima of probes that were measured in CH_2Cl_2 (λ_{em1}) and upon interaction with Aβ_{1-42} aggregates in PBS (λ_{em2}). [b]Quantum yields that were measured in CH_2Cl_2 and PBS, respectively. [c]Fluorescence enhancement after binding to Aβ_{1-42} aggregates in PBS. [d]K_d values to Aβ_{1-42} aggregates measured in triplicate with results given as mean ± standard deviation (SD). [e]Calculated using the online ALOGPS 2.1 program. [f]Rotation energies were calculated using the B3LYP/6-31G* method in CH_2Cl_2.

Scheme 1. Synthesis of the DANIR Probes[a]

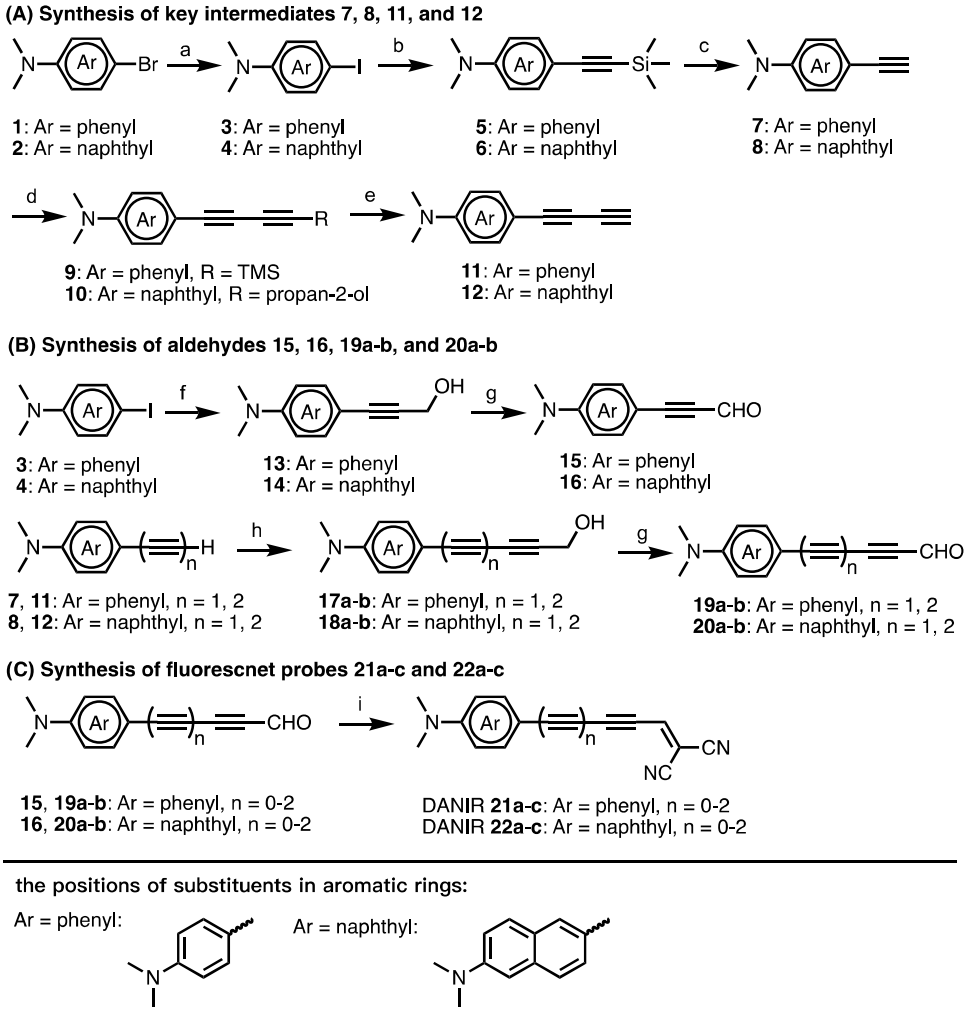

[a]Reagent and conditions: (a) (1) *n*-BuLi (1.6 M in hexane), anhydrous tetrahydrofuran (THF), −78 °C, 30 min, (2) I_2, room temperature (rt), 30 min; (b) $PdCl_2(PPh_3)_2$ for **5** or $Pd(PPh_3)_4$ for **6**, CuI, triethylamine (Et_3N), THF, 66 °C, 24 h; (c) tetrabutylammonium fluoride (TBAF), THF, 66 °C, 3 h; (d) ethynyltrimethylsilane, Cu, and CH_2Cl_2/1,4-dioxane (v/v = 3/1) for **9** or 3-butyn-2-ol, CuCl, and $CHCl_3$ for **10**, tetramethylethylenediamine (TMEDA), O_2, 50 °C, overnight; (e) TBAF and THF for **11** or NaOH and 1,4-dioxane for **12**, 66 °C, 3 h; (f) $PdCl_2(PPh_3)_2$ for **13** or $Pd(PPh_3)_4$ for **14**, ethynol, CuI, Et_3N, THF, N_2, rt, overnight; (g) Dess−Martin periodinane reagent (DMP), CH_2Cl_2, rt, 10 min; (h) ethynol, Cu, TMEDA, O_2, CH_2Cl_2/1,4-dioxane (v/v = 3/1), 50 °C; (i) malononitrile, basic Al_2O_3 (48−75 μm), CH_2Cl_2, rt, 5 min.

plaques with improved properties like high quantum yield (QY, 9.0% in dichloromethane (DCM), 0.009% in phosphate-buffered saline (PBS)) and a high affinity (K_d = 1.9 nM).[11,17]

In general, these intramolecular charge transfer (ICT) probes (Figure 1A) share a common D−π−A structure, consisting of an electron donor (D) group and an electron acceptor (A) group, which were connected by a conjugated π bridge (π).[18−20] As

https://dx.doi.org/10.1021/acs.jpcb.0c08845
J. Phys. Chem. B 2021, 125, 497−506

reported, the biological and optical properties of these probes could be efficiently tuned by adjusting the number of conjugated C═C units.[21] However, the C═C bonds could be isomerized under light irradiation, which may cause a change in the molecular conformation in solvent and thus deteriorate their performance when binding to Aβ plaques. Moreover, these probes are very sensitive to the polarity of the surrounding environment. Their quantum yields were remarkably increased when the solvent altered from polar PBS to nonpolar DCM (e.g., DANIR **2c** and **3c**, Table 1), which may likely induce severe nonspecific signals when used in *in vivo* brain imaging.[17,22]

Similar to the C═C bond, polyacetylene chain also possesses excellent electron transfer capability and has been widely used in the chemo-sensors of many fields like polarity, viscosity, NO, and oxygen.[23−25] In 2015, Whitten's and Chi's group developed a focused library of molecular rotors based on the phenylene ethylene backbone, which demonstrated moderate increases in fluorescence intensity after incubated with hen egg-white lysozyme-induced amyloid conformer, and the lowest binding constant was determined as 1 μM.[26,27] The polyacetylene chain endows the probes with distinctive design features (Figure 1B): (1) Since the C≡C bond is formed by sp hybridization between two carbon atoms, its derivatives often share a linear structure, in which the terminal moieties could rotate freely around the polyacetylene π bridge. (2) The polyacetylene chain is an excellent π bridge in D−π−A molecules.[28] The emission maximum of a fluorescent probe might be shifted to the NIR window with the extension of the polyacetylene chain. (3) Besides, the probe with polyacetylene chains could avoid isomerization, which may result in a more precise response to Aβ plaques. Herein, we designed and synthesized a focused library of D−π−A fluorescent probes (**21a−c** and **22a−c**, Scheme 1) that contain polyacetylene chains as conjugated π bridges. Furthermore, these compounds were assessed as NIR probes for the detection of Aβ plaques *in vitro*.

2. METHODS

2.1. General Information. All reagents used for synthesis were of commercial grade and used without further purification. Thin-layer chromatography (TLC) was used for monitoring reactions on Merck silica gel 60 F_{254} plates. Upon loading to the flash column (Silica-CS, 40−60 μm, 20−80 g, Bonna-Agela Technologies Co., Ltd., China), the compounds in organic synthesis were purified using a FLEXA modular preparative chromatography system (Bonna-Agela Technologies Co., Ltd., China). Amyloid-β_{1-42} peptides were purchased from Peptide Institute, Inc. (Japan) and aggregated and tested by the reported method.[29] ^{1}H and ^{13}C NMR spectra were collected on a Bruker Avance III (400 for ^{1}H or 100 MHz for ^{13}C, respectively, 5 mm PABBO BB- probe), a JEOL JNM-ECZ400R/S1 (400 for ^{1}H or 100 MHz for ^{13}C, respectively, 4 mm Cryocoil MAS probe), or a JNMECZ600R/S3 (600 for ^{1}H or 150 MHz for ^{13}C, respectively, 4 mm Cryocoil MAS probe) NMR spectrometer in $CDCl_3$, trifluoroacetic acid-*d*, or dimethyl sulfoxide (DMSO)-d_6 at room temperature unless further noted. Chemical shifts were reported in parts per million (ppm) compared with tetramethylsilane (δ 0.00, s). Coupling constants (J) were reported in hertz (Hz). Multiplicities were reported as s (singlet,), d (doublet), t (triplet), and m (multiplet). Mass spectrometry (MS) spectra were acquired on a Thermo Scientific LCQ FLEET (electrospray ionization (ESI)) mass spectrometer. High-resolution mass spectra were acquired on a Thermo Scientific Q Exactive (ESI) mass spectrometer. UV−visible (UV−vis) spectra were obtained on a Shimadzu UV-2450 UV−vis spectrophotometer (Japan) with a Jiangsu Jingbo quartz absorption cell (751, 10 mm). Fluorescence spectra were recorded on a Shimadzu RF-5301PC spectrofluorophotometer (Japan) with a Jiangsu Jingbo quartz absorption cell (751, 10 mm). Fluorescence QYs were measured on a Hamamatsu C11347 Absolute PL quantum yield spectrometer (Japan). High-performance liquid chromatography (HPLC) was performed on a Hitachi Primaide system (Japan). Samples were analyzed on a Bonna-Agela Technologies Venusil MP C18 reverse-phase column (5 μm, 4.6 mm × 250 mm) and eluted at a flow rate of 1.0 mL/min. Mobile phase A was water, and mobile phase B was acetonitrile. *In vitro* fluorescent staining results were acquired on a Life Technologies EVOS FL imaging system (equipped with DAPI, GFP, RFP, and CY5 filter sets) or a Leica DMi8 THUNDER (equipped with DAPI, GFP, and RFP filter sets, Germany). Alzheimer's model mouse (C57BL6, APPsw/PSEN1, 13 months old, male) were purchased from the Institute of Laboratory Animal Sciences, Chinese Academy of Medical Sciences (Beijing, P. R. China), and the mouse brain was used to prepare paraffin sections after sacrifice. The brain tissues of autopsy-confirmed AD patients (95 years old, female; 64 years old, female) were obtained from the Chinese Brain Bank Center (CBBC), South-Central University for Nationalities (Wuhan, P. R. China).

2.2. Chemistry. *2.2.1. 4-Iodo-N,N-dimethylaniline (**3**).* To a stirred solution of **1** (10.0 g, 50 mmol) in anhydrous THF, *n*-butyllithium (40 mL, 1.6 M hexane, 64 mmol) was added dropwise at −78 °C under nitrogen atmosphere. The mixture was stirred for 30 min. Afterward, iodine (13.9 g, 55 mmol) was dissolved in anhydrous THF and added into the above mixture, stirred at room temperature for an additional 30 min, and then the reaction was neutralized by saturated $Na_2S_2O_3$ aqueous solution. THF was removed under vacuum, and the residue was extracted with petroleum ether (3 × 100 mL). The combined organic layer was dried over anhydrous Na_2SO_4, and solvents were evaporated under vacuum to yield **3** as a white crystalline solid without further purification (12.2 g, 98.5%). ^{1}H NMR (400 MHz, $CDCl_3$) δ 7.47 (d, J = 8.4 Hz, 2H), 6.51 (d, J = 8.4 Hz, 2H), 2.92 (s, 6H). Spectra data are consistent with the literature.[30]

*2.2.2. N,N-Dimethyl-4-((trimethylsilyl)ethynyl)aniline (**5**).* The preparation of compound **5** was in accordance with a reported study with slight modification.[31] To a stirred solution of **3** (2.0 g, 8.0 mmol) in THF, $PdCl_2(PPh_3)_2$ (168.5 mg, 0.24 mmol), CuI (91.4 mg, 0.48 mmol), and Et_3N (1.7 mL, 12.0 mmol) were added, and finally the solution of ethynyltrimethylsilane in THF was added slowly under nitrogen atmosphere. The reaction mixture was maintained for 24 h at room temperature. The mixture was filtered, and the solvent was removed by vacuum. The residue was purified by flash column chromatography (petroleum ether/CH_2Cl_2 = 3/1, v/v) to give **5** as a pale yellow solid (1.2 g, 66.7%). ^{1}H NMR (600 MHz, $CDCl_3$) δ 7.33 (d, J = 8.6 Hz, 2H), 6.59 (d, J = 8.6 Hz, 2H), 2.96 (s, 6H), 0.22 (s, 9H).

*2.2.3. 4-Ethynyl-N,N-dimethylaniline (**7**).* The preparation of compound **7** was in accordance with a reported study with slight modification.[31] To a solution of **5** (1.1 g, 5.3 mmol) in THF, tetrabutylammonium fluoride (TBAF, 10.6 mL, 1 M in THF, 10.6 mmol) was added, and the mixture was refluxed for 3 h. After cooling to room temperature, the mixture was washed with water and extracted with CH_2Cl_2 (3 × 100 mL). The combined organic layer was dried over anhydrous Na_2SO_4,

https://dx.doi.org/10.1021/acs.jpcb.0c08845
J. Phys. Chem. B 2021, 125, 497−506

concentrated, and purified by flash column chromatography (petroleum ether/CH_2Cl_2 = 9/1, v/v) to give **7** as a pale yellow solid (566.8 mg, 73.6%). ^{1}H NMR (600 MHz, $CDCl_3$) δ 7.38 (d, J = 8.9 Hz, 2H), 6.61 (d, J = 8.9 Hz, 2H), 2.98 (s, 6H).

*2.2.4. N,N-Dimethyl-4-((trimethylsilyl)buta-1,3-diyn-1-yl)-aniline (**9**).* The preparation of compound **9** was in accordance with a reported study with slight modification.[28] A mixture of copper powder (6.4 mg, 0.1 mmol) and tetramethylethylenediamine (TMEDA, 46.5 mg, 0.4 mmol) in the mixed solution of CH_2Cl_2 and 1,4-dioxane (v/v = 3/1) was stirred under air for 2 min. Then, compound **7** (290.4 mg, 2 mmol) and ethynyltrimethylsilane (0.15 mL, 2.6 mmol) were added slowly. The reaction mixture was stirred at 50 °C and monitored by TLC. After consumption of the starting material, the mixture was filtered and concentrated under vacuum. The crude product was further purified by flash column chromatography (petroleum ether/CH_2Cl_2 = 5/1, v/v) to give **9** as a tawny solid (52.3 mg, 10.8%). ^{1}H NMR (400 MHz, $CDCl_3$) δ 7.35 (d, J = 8.8 Hz, 2H), 6.59 (d, J = 8.8 Hz, 2H), 2.98 (s, 6H), 0.20 (s, 9H).

*2.2.5. 4-(Buta-1,3-diyn-1-yl)-N,N-dimethylaniline (**11**).* The same reaction described above to prepare compound **7** was used, and the crude product was purified by flash column chromatography (petroleum ether/ethyl acetate = 3/1, v/v). Compound **11** was obtained as a pale yellow solid (91.5 mg, 87.1%). ^{1}H NMR (600 MHz, $CDCl_3$) δ 7.37 (d, J = 6.4 Hz, 2H), 6.75 (d, J = 6.4 Hz, 2H), 3.85 (s, 6H), 3.42 (s, 1H). MS found 170.2; molecular formula $C_{12}H_{11}N$ requires $[M + H]^+$ 170.1

*2.2.6. 3-(4-(Dimethylamino)phenyl)prop-2-yn-1-ol (**13**).* To a stirred solution of **3** (1.2 g, 5.0 mmol) and ethynol (364.5 mg, 6.5 mmol) in THF, $PdCl_2(PPh_3)_2$ (175.7 mg, 0.25 mmol), CuI (47.6 mg, 0.25 mmol), and Et_3N (87.6 mg, 0.5 mmol) were added. The reaction mixture was maintained for 24 h at room temperature under nitrogen atmosphere. The mixture was filtered, and the solvent was removed by vacuum. The crude product was purified by flash column chromatography (petroleum ether/ethyl acetate = 9/1, v/v). Compound **13** was obtained as a yellow solid (1305.4 mg, 52.8%). ^{1}H NMR (400 MHz, $CDCl_3$) δ 7.30 (d, J = 8.8 Hz, 2H), 6.61 (d, J = 8.8 Hz, 2H), 4.47 (d, J = 5.5 Hz, 2H), 2.96 (s, 6H). Spectra data are consistent with the literature.[32]

*2.2.7. 3-(4-(Dimethylamino)phenyl)propiolaldehyde (**15**).* The preparation of compound **15** was in accordance with a reported study with slight modification.[28] To a solution of **13** (697.7 mg, 4.0 mmol) in CH_2Cl_2, Dess−Martin periodinane (DMP, 1703.5 mg, 4 mmol) was added in batches. The reaction was stirred at room temperature and monitored by TLC. After the reaction was finished, saturated Na_2SO_3 aqueous solution and $NaHCO_3$ aqueous solution were added. The resulting mixture was extracted with CH_2Cl_2 (3 × 100 mL) and dried over anhydrous Na_2SO_4. The solvent was evaporated under vacuum, and the residue was purified by flash column chromatography (petroleum ether/CH_2Cl_2 = 3/1, v/v) to give **15** as a yellow solid (34.1 mg, 5%).

*2.2.8. 5-(4-(Dimethylamino)phenyl)penta-2,4-diyn-1-ol (**17a**).* The same reaction described above to prepare compound **9** was used, and the crude product was purified by flash column chromatography (petroleum ether/ethyl acetate = 3/1, v/v). Compound **17a** was obtained as a pale yellow solid (50.3 mg, 12.6%). ^{1}H NMR (400 MHz, $CDCl_3$) δ 7.36 (d, J = 8.8 Hz, 2H), 6.60 (d, J = 8.8 Hz, 2H), 4.40 (s, 2H), 2.99 (s, 6H).

*2.2.9. 5-(4-(Dimethylamino)phenyl)penta-2,4-diynal (**19a**).* The same reaction described above to prepare compound **15** was used, and the crude product was purified by flash column chromatography (petroleum ether/ethyl acetate = 3/1, v/v). Compound **19a** was obtained as a pale yellow solid (95.0 mg, 53.0%). ^{1}H NMR (400 MHz, $CDCl_3$) δ 9.26 (s, 1H), 7.43 (d, J = 9.3 Hz, 2H), 6.60 (d, J = 9.3 Hz, 2H), 3.02 (s, 6H).

*2.2.10. 7-(4-(Dimethylamino)phenyl)hepta-2,4,6-triyn-1-ol (**17b**).* The same reaction described above to prepare compound **9** was used, and the crude product was purified by flash column chromatography (petroleum ether/ethyl acetate = 6/1, v/v). Compound **17b** was obtained as a saffron yellow solid (44.2 mg, 33.6%). ^{1}H NMR (400 MHz, $CDCl_3$) δ 7.39 (d, J = 8.8 Hz, 2H), 6.62 (d, J = 8.8 Hz, 12H), 4.37 (s, 2H), 3.00 (s, 6H). Spectra data are consistent with the literature.[28]

*2.2.11. 17-(4-(Dimethylamino)phenyl)hepta-2,4,6-triynal (**19b**).* The same reaction described above to prepare compound **15** was used, and the crude product was purified by flash column chromatography (petroleum ether/ethyl acetate = 5/1, v/v). Compound **19b** was obtained as a pale yellow solid (42.3 mg, 47.8%). ^{1}H NMR (400 MHz, $CDCl_3$) δ 9.22 (s, 1H), 7.43 (d, J = 9.1 Hz, 2H), 6.60 (d, J = 9.1 Hz, 2H), 3.02 (s, 6H).

*2.2.12. 2-(3-(4-(Dimethylamino)phenyl)prop-2-yn-1-ylidene) malononitrile (**21a**).* To a solution of **15** (34.1 mg, 0.2 mmol) in CH_2Cl_2, malononitrile and basic Al_2O_3 (48−75 μm, Sinopharm Chemical Reagent Beijing Co., Ltd.) was added.[33] The reaction finished at once. The crude product was purified by flash column chromatography (pure CH_2Cl_2) and recrystallization in petroleum ether. Compound **21a** was obtained as red-purple crystalline solid (42.3 mg, 95.7%). ^{1}H NMR (400 MHz, $CDCl_3$) δ 7.51 (d, J = 8.9 Hz, 2H), 7.09 (s, 1H), 6.69 (d, J = 8.9 Hz, 2H), 3.08 (s, 6H). ^{13}C NMR (101 MHz, $CDCl_3$) δ 152.52, 141.07, 135.57, 121.60, 113.62, 112.39, 111.73, 105.74, 88.29, 40.03. HRMS found 222.1022; molecular formula $C_{14}H_{11}N_3$ requires $[M + H]^+$ 222.0953. Spectra data are consistent with the literature.[28]

*2.2.13. 2-(5-(4-(Dimethylamino)phenyl)penta-2,4-diyn-1-ylidene)malononitrile (**21b**).* The same reaction described above to prepare compound **21a** was used, and the crude product was purified by flash column chromatography (pure CH_2Cl_2). Compound **21b** was obtained as a dark purple crystalline solid (44.1 mg, 90.0%). ^{1}H NMR (400 MHz, $CDCl_3$) δ 7.48 (d, 2H), 7.01 (s, 1H), 6.63 (d, J = 9.0 Hz, 2H), 3.05 (s, 6H). ^{13}C NMR (101 MHz, $CDCl_3$) δ 151.73, 140.43, 135.24, 112.81, 112.07, 111.64, 105.93, 101.51, 100.02, 93.86, 73.55, 40.29. HRMS found 246.1024; molecular formula $C_{16}H_{11}N_3$ requires $[M + H]^+$ 246.0953. Spectra data are consistent with the literature.[28]

*2.2.14. 2-(7-(4-(Dimethylamino)phenyl)hepta-2,4,6-triyn-1-ylidene)malononitrile (**21c**).* The same reaction described above to prepare compound **21a** was used, and the crude product was purified by flash column chromatography (pure CH_2Cl_2). Compound **21c** was obtained as a dark purple crystalline solid (40.0 mg, 78.2%). ^{1}H NMR (600 MHz, $CDCl_3$) δ 7.44 (d, J = 9.1 Hz, 2H), 6.96 (s, 1H), 6.64 (d, J = 9.0 Hz, 2H), 3.04 (s, 6H). ^{13}C NMR (101 MHz, Trifluoroacetic Acid-d) δ 143.02, 142.33, 135.31, 123.97, 120.04, 98.83, 95.84, 81.58, 78.35, 74.71, 70.08, 63.87, 46.94. HRMS found 270.1023; molecular formula $C_{18}H_{11}N_3$ requires $[M + H]^+$ 270.0953. Spectra data are consistent with the literature.[28]

*2.2.15. 6-Iodo-N,N-dimethylnaphthalen-2-amine (**4**).* The same reaction described above to prepare compound **3** was used, and the crude product was purified by flash column chromatography (petroleum ether/ethyl acetate = 3/1, v/v) to give **4** as a pale yellow solid (574.7 mg, 64.5%). MS found 298.3; molecular formula $C_{12}H_{12}IN$ requires $[M + H]^+$ 298.0.

https://dx.doi.org/10.1021/acs.jpcb.0c08845
J. Phys. Chem. B 2021, 125, 497−506

*2.2.16. N,N-Dimethyl-6-((trimethylsilyl)ethynyl)-naphthalen-2-am-5ine (**6**).* The same reaction described above to prepare compound **5** was used. Compound **6** was obtained as a tawny solid (40.0 mg, 78.2%). ^{1}H NMR (400 MHz, $CDCl_3$) δ 7.88 (s, 1H), 7.70 (s, 1H), 7.60 (s, 1H), 7.44 (s, 1H), 6.99 (s, 1H), 3.10 (s, 6H), 0.27 (s, 9H). MS found 268.3; molecular formula $C_{17}H_{21}NSi$ requires $[M + H]^+$ 268.1. Spectra data are consistent with the literature.[34]

*2.2.17. 6-Ethynyl-N,N-dimethylnaphthalen-2-amine (**8**).* The same reaction described above to prepare compound **7** was used, and the crude product was purified by flash column chromatography (petroleum ether/ethyl acetate = 1/1, v/v). Compound **8** was obtained as a pale yellow solid (292.5 mg, 15.0%). ^{1}H NMR (400 MHz, $CDCl_3$) δ 7.91 (s, 1H), 7.71 (s, 1H), 7.63 (s, 1H), 7.47 (s, 1H), 6.99 (s, 1H), 3.11 (s, 6H). Spectra data are consistent with the literature.[34]

*2.2.18. 6-(6-(Dimethylamino)naphthalen-2-yl)-2-methylhexa-3,5-diyn-2-ol (**10**).* To a solution of **8** (366 mg, 19 mmol) and 3-butyn-2-ol (236.9 mg, 1.9 mmol) in $CHCl_3$, CuCl (9.3 mg, 0.09 mmol) and TMEDA (43.7 mg, 0.4 mmol) were added. The reaction mixture was stirred at 50 °C for 4 h and monitored by TLC. The solvent was evaporated under vacuum, and the residue was purified by flash column chromatography (petroleum ether/ethyl acetate = 5/1, v/v) to give **10** as a pale yellow solid (364.8 mg, 70.2%).

*2.2.19. 6-(Buta-1,3-diyn-1-yl)-N,N-dimethylnaphthalen-2-amine (**12**).* To a solution of **10** (345.7 mg, 1.3 mmol) in 1,4-dioxane, NaOH (105.6 mg, 2.64 mmol) was added. The reaction mixture was refluxed at 60 °C and monitored by TLC. The above mixture was filtered, and the residue was purified by flash column chromatography (petroleum ether/CH_2Cl_2 = 2/1, v/v) to give **12** was obtained as a pale yellow solid (148.2 mg, 54.1%). ^{1}H NMR (400 MHz, $CDCl_3$) δ 7.90 (s, 1H), 7.65 (d, J = 9.1 Hz, 1H), 7.56 (d, J = 8.5 Hz, 1H), 7.40 (dd, J = 8.5, 1.5 Hz, 1H), 7.16 (d, J = 8.0 Hz, 1H), 6.85 (s, 1H), 3.08 (s, 6H), 2.49 (s, 1H). MS found 220.3; molecular formula $C_{16}H_{13}N$ requires $[M + H]^+$ 220.1.

*2.2.20. 3-(6-(Dimethylamino)naphthalen-2-yl)prop-2-yn-1-ol (**14**).* The same reaction described above to prepare compound **13** was used, and the crude product was purified by flash column chromatography (petroleum ether/ethyl acetate = 3/1, v/v). Compound **14** was obtained as a tawny oil (170.0 mg, 39.7%). ^{1}H NMR (400 MHz, $CDCl_3$) δ 7.79 (s, 1H), 7.63 (d, J = 9.1 Hz, 1H), 7.55 (d, J = 8.5 Hz, 1H), 7.34 (dd, J = 8.5, 1.6 Hz, 1H), 7.13 (dd, J = 9.1, 2.5 Hz, 1H), 6.85 (s, 1H), 4.51 (s, 2H), 3.05 (s, 6H).

*2.2.21. 3-(6-(Dimethylamino)naphthalen-2-yl)-propiolaldehyde (**16**).* The same reaction described above to prepare compound **15** was used, and the crude product was purified by flash column chromatography (petroleum ether/ethyl acetate = 6/1, v/v). Compound **16** was obtained as a pale yellow solid (50.2 mg, 12.9%). ^{1}H NMR (400 MHz, $CDCl_3$) δ 9.44 (s, 1H), 8.04 (s, 1H), 7.73 (d, J = 9.1 Hz, 1H), 7.63 (d, J = 8.5 Hz, 1H), 7.48 (d, J = 8.5 Hz, 1H), 7.23 (d, J = 9.1 Hz, 1H), 6.99 (s, 1H), 3.12 (s, 6H). MS found 224.3; molecular formula $C_{15}H_{13}NO$ requires $[M + H]^+$ 224.1.

*2.2.22. 5-(6-(Dimethylamino)naphthalen-2-yl)penta-2,4-diyn-1-ol (**18a**).* The same reaction described above to prepare compound **9** was used, and the crude product was purified by flash column chromatography (petroleum ether/ethyl acetate = 3/1, v/v). Compound **18a** was obtained as a brown solid (331.0 mg, 88.6%). ^{1}H NMR (400 MHz, $CDCl_3$) δ 7.93 (s, 1H), 7.72 (s, 1H), 7.64 (s, 1H), 7.44 (d, J = 7.4 Hz, 1H), 7.29 (s, 1H), 4.44 (s, 2H), 3.13 (s, 6H).

*2.2.23. 5-(6-(Dimethylamino)naphthalen-2-yl)penta-2,4-diynal (**20a**).* The same reaction described above to prepare compound **15** was used. Compound **20a** was obtained as a reddish-brown solid (55.6 mg, 26.4%). ^{1}H NMR (400 MHz, $CDCl_3$) δ 9.30 (s, 1H), 8.00 (s, 1H), 7.72 (d, J = 9.0 Hz, 1H), 7.63 (d, J = 8.5 Hz, 1H), 7.45 (d, J = 8.7 Hz, 1H), 7.06 (s, 1H), 3.13 (s, 6H).

*2.2.24. 7-(6-(Dimethylamino)naphthalen-2-yl)hepta-2,4,6-triyn-1-ol (**18b**).* The same reaction described above to prepare compound **9** was used, and the crude product was purified by flash column chromatography (petroleum ether/ethyl acetate = 3/1, v/v). Compound **18b** was obtained as a brown solid (17.0 mg, 14.1%).

*2.2.25. 7-(6-(Dimethylamino)naphthalen-2-yl)hepta-2,4,6-triynal (**20b**).* The same reaction described above to prepare compound **15** was used. Compound **20b** was obtained as a reddish-brown solid (55.6 mg, 26.4%). ^{1}H NMR (400 MHz, $CDCl_3$) δ 9.14 (s, 1H), 7.87 (s, 1H), 7.59−7.51 (m, 1H), 7.46 (d, J = 8.5 Hz, 1H), 7.30 (d, J = 8.5 Hz, 1H), 7.06 (d, J = 9.0 Hz, 1H), 6.75 (s, 1H), 3.00 (s, 6H).

*2.2.26. 2-(3-(6-(Dimethylamino)naphthalen-2-yl)prop-2-yn-1-ylidene)malononitrile (**22a**).* The same reaction described above to prepare compound **21a** was used, and the crude product was purified by flash column chromatography (pure CH_2Cl_2). Compound **22a** was obtained as an orange red crystalline solid (24.9 mg, 9.2%). ^{1}H NMR (400 MHz, $CDCl_3$) δ 8.04 (s, 1H), 7.75 (d, J = 8.4 Hz, 1H), 7.64 (d, J = 6.7 Hz, 1H), 7.46 (d, J = 8.5 Hz, 1H), 7.22 (s, 1H), 7.17 (s, 1H), 6.99 (s, 1H), 3.15 (s, 6H). ^{13}C NMR (101 MHz, $CDCl_3$) δ 141.15, 136.61, 135.45, 130.09, 128.94, 126.80, 125.81, 119.17, 116.63, 113.13, 111.98, 106.26, 90.93, 86.82, 77.23, 40.71. HRMS found 272.1179; molecular formula $C_{18}H_{13}N_3$ requires $[M + H]^+$ 272.1109.

*2.2.27. 2-(5-(6-(Dimethylamino)naphthalen-2-yl)penta-2,4-diyn-1-ylidene)malononitrile (**22b**).* The same reaction described above to prepare compound **21a** was used, and the crude product was purified by flash column chromatography (pure CH_2Cl_2). Compound **22b** was obtained as a brown-purple crystalline solid (24.9 mg, 90.6%). ^{1}H NMR (400 MHz, $CDCl_3$) δ 8.02 (s, 1H), 7.72 (d, J = 9.1 Hz, 1H), 7.63 (d, J = 8.6 Hz, 1H), 7.45 (d, J = 8.7 Hz, 1H), 7.23 (s, 1H), 7.04 (s, 1H), 6.99 (s, 1H), 3.13 (s, 6H). ^{13}C NMR (101 MHz, $CDCl_3$) δ 140.41, 136.27, 135.06, 129.63, 128.79, 126.66, 125.56, 116.66, 112.60, 111.84, 111.45, 105.64, 100.32, 98.60, 95.10, 75.94, 73.23, 40.54. HRMS found 296.1179; molecular formula $C_{20}H_{13}N_3$ requires $[M + H]^+$ 296.1109.

*2.2.28. 2-(7-(6-(Dimethylamino)naphthalen-2-yl)hepta-2,4,6-triyn-1-ylidene)malononitrile (**22c**).* The same reaction described above to prepare compound **21a** was used, and the crude product was purified by flash column chromatography (pure CH_2Cl_2). Compound **22c** was obtained as a dark purple crystalline solid (3.0 mg, 23.5%). ^{1}H NMR (400 MHz, $CDCl_3$) δ 7.99 (s, 1H), 7.69 (d, J = 9.0 Hz, 1H), 7.59 (d, J = 8.5 Hz, 1H), 7.42 (d, J = 8.4 Hz, 1H), 7.21 (d, J = 8.5 Hz, 1H), 6.97 (s, 2H), 3.12 (s, 6H). ^{13}C NMR (101 MHz, $CDCl_3$) δ 139.55, 135.81, 134.96, 129.52, 129.00, 126.77, 116.77, 112.16, 111.01, 98.79, 97.20, 89.04, 88.74, 86.33, 80.85, 77.27, 73.73, 71.60, 64.81, 40.94. HRMS: m/z calcd for $[M + H]^+$ 320.1109, found 320.1179. HRMS found 320.1179; molecular formula $C_{22}H_{13}N_3$ requires $[M + H]^+$ 320.1109.

https://dx.doi.org/10.1021/acs.jpcb.0c08845
J. Phys. Chem. B 2021, 125, 497−506

2.3. Spectroscopic Measurements. Ultraviolet absorption spectra and fluorescence spectra of probes were recorded according to the previously reported methods,[29] and the experimental details are given in the Supporting Information (SI).

2.4. Biological Evaluations. For these new probes, the fluorescent responses with Aβ_{1-42} aggregates and bovine serum albumin (BSA), binding affinity to Aβ_{1-42} aggregates, *in vitro* fluorescent staining on brain sections of transgenic mice and AD patients, and NMR titration were tested according to the previously reported methods,[29,35,36] and the detailed procedures are given in the SI.

3. RESULTS

3.1. Synthesis. The synthetic routes of the final products (**21a−c** and **22a−c**) are shown in Scheme 1. Briefly, the arylacetylenes (**7** and **8**) were synthesized by the Sonogashira cross-coupling from the corresponding iodinated compounds (**3** and **4**). In the following, Glaser and Hay couplings were used to prolong the polyacetylene chain (n = 1−3) to obtain corresponding compounds (**9**, **10**, **17a−b**, and **18a−b**) in moderate to high yields (33.9−88.6%). Then, the terminal alcohols (**13**, **14**, **17a−b**, and **18a−b**) were oxidized to aldehydes (**15**, **16**, **19a−b**, and **20a−b**) by Dess−Martin periodinane reagent. The final probes (**21a−c** and **22a−c**) were prepared by Knoevenagel condensation from the aldehydes (**15**, **16**, **19a−b**, and **20a−b**) and malononitrile with low to high yield (9.2−95.7%) using basic Al_2O_3 as a base catalyst. All of the final probes were purified by flash column chromatography and recrystallization in the petroleum ether/CH_2Cl_2 system and fully characterized by ^{1}H NMR, ^{13}C NMR, and high-resolution mass spectrometry (HRMS), and the spectra were given in the SI. Their purities were determined to be greater than 95% by analytical HPLC (Figure S1 and Table S1 in the SI).

3.2. Fluorescence Properties. In general, D−π−A-based molecules have typical ICT characteristics that the delocalization effect of electrons could be enhanced by the extension of the conjugated π system, which results in a higher electron density in the electron acceptor moiety and a red shift of the fluorescent emission wavelength.[37,38] In this case, the chemical shifts of the hydrogen in acceptor moiety (Figure 2, indicated by asterisks) displayed gradual upfield shifts (from 7.09 to 6.96 ppm for **21a−c** and 7.17 to 6.97 ppm for **22a−c**) in ^{1}H NMR spectra, indicating that the electron density of acceptor moiety increased with the expansion of the C≡C units.

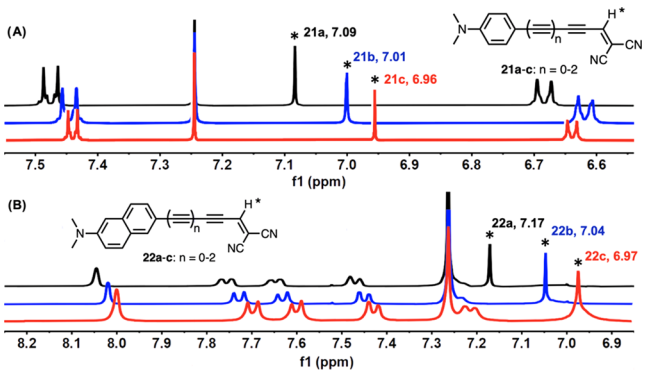

Figure 2. Chemical shifts (ppm) of the ethylenic hydrogens (indicated by asterisks) of compounds **21a−c** (A) and **22a−c** (B) in ^{1}H NMR (600 MHz) spectra. All spectra were recorded in DMSO-d_6 solution at room temperature. The asterisks indicate the ethylenic hydrogens and their corresponding peaks.

As shown in Table 1, the anticipated increase in the fluorescent maxima of these probes was not observed with the extension of polyacetylene chain, which is different from the reported ICT probes with polyene chains.[11,17,21] For phenyl derivatives (**21a−c**), **21c** with the largest conjugated π system displayed the longest emission maximum at 649 nm, while **21a** and **21b** showed nearly the same maxima around 580 nm. In addition, the naphthalene derivatives (**22a−c**) exhibited irregular fluorescent properties that **22a** had the longest emission wavelength of 627 nm in dichloromethane followed by **22c** and **22b** (596 and 520 nm, respectively). Moreover, all of these new probes displayed shorter emission maxima (<650 nm) than those of DANIR **2c** and **3c** (660 and 720 nm, respectively, Table 1). These results may be caused by both charge delocalization and molecule configuration: (1) The electrons are held more firmly by carbon atoms in C≡C bonds (sp hybridization) than in C=C bonds (sp^2 hybridization), and their transformation is obstructed in a polyacetylene chain, which expands the highest occupied molecular orbital−lowest unoccupied molecular orbital (HOMO−LUMO) gap and leads to a blue shift in emission maximum. (2) For our new probes, an obvious decrease in the rotation energy barrier (1.88−6.28 eV, Table 1) was observed compared with that of polyene probes DANIR **2c** and **3c** (>16 eV, Table 1), which leads to multiple molecular rotations in free status and thus influenced the excited-state dipole (Figure S2 and S3 in the SI).[17,39] Furthermore, in the solvents of nonpolar dichloromethane and polar PBS, which have significantly different polarities, each probe displayed very similar fluorescent quantum yields (0.2−1.8%, Table 1), indicating that the QYs of our probes are nonsensitive to the microenvironment when in their free state. This result is different from the QYs of DANIR **2c** and **3c**, which have large increases (21- and 1000-fold, respectively, Table 1) when the solvent transferred from PBS to DCM.[11,17]

3.3. Fluorescent Responses upon Interaction with Aβ_{1-42} Aggregates. An ICT probe usually displays obvious fluorescent responses after binding to Aβ_{1-42} aggregates, including blue shift of emission maximum and increase in fluorescence intensity.[11,17,21] As shown in Table 1, after the incubation with Aβ_{1-42} aggregates, the emission maxima of our probes increased with the extension of polyacetylene chain. Among them, three of the probes, **21c**, **22b**, and **22c**, displayed long emission maxima of 649, 650, and 665 nm, respectively, which are suitable for *in vivo* NIR imaging. Furthermore, a significant increase in fluorescence intensity (45- to 360-fold, Table 1 and Figure 3) was observed, which may be caused by that the probe was forced to adapt an inflexible structure with restricted rotational motion after inserted into the binding pocket of Aβ_{1-42} aggregates, and thus the nonradiative decay was forbade and the energy was depleted by fluorescence emitting. Of note, unlike the irregular emission wavelength shift in free status, an obvious red shift was observed with increasing number of C≡C units (from 535 to 649 nm for benzene derivatives **21a−c**, and from 603 to 665 nm for naphthalene derivatives **22a−c**; Table 1) after incubating with Aβ_{1-42} aggregates. As hindered by the binding pocket, the rotation of the new probes was minimized, and these molecules were promoted a rigid configuration, which makes the length of the π system a dominant factor in regulating the fluorescence maxima. In addition, the fluorescent response also suggested that no interaction occurred between our probes and BSA (Figure 3).

https://dx.doi.org/10.1021/acs.jpcb.0c08845
J. Phys. Chem. B 2021, 125, 497−506

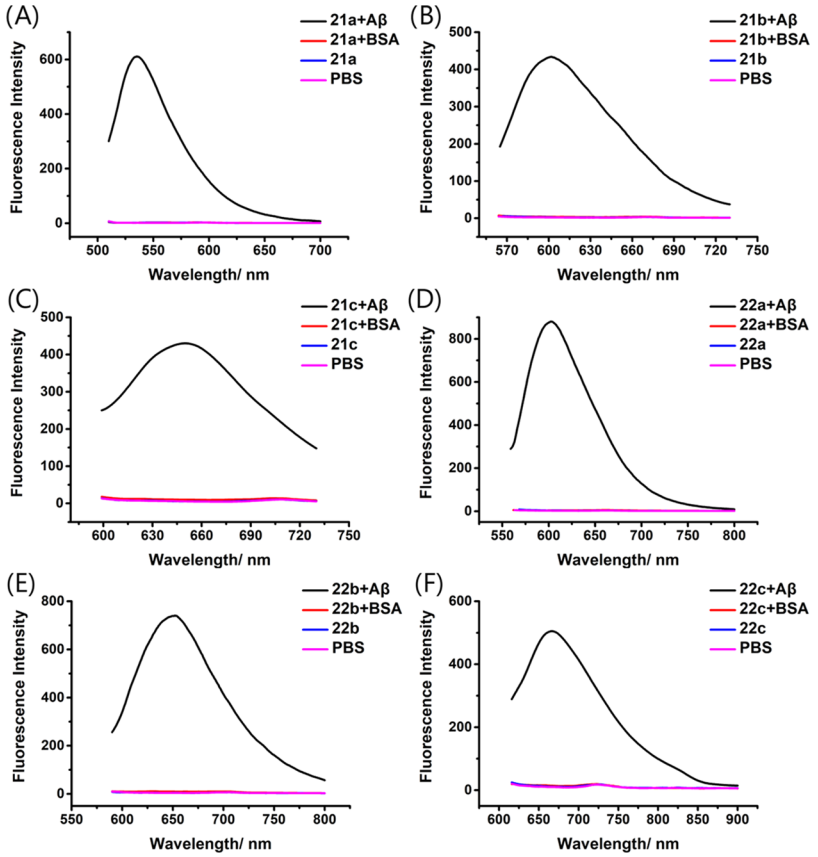

Figure 3. Fluorescence emission spectra of **21a−c** (A−C, respectively) and **22a−c** (D−F, respectively) upon interaction with Aβ_{1-42} aggregates (10 μg/mL, black line) or BSA (10 μg/mL, red line). The spectra of the compound in PBS (50 nM, blue line) and PBS alone (pink line) were recorded in the same condition.

Taken together, in free status, our new probes are insensitive to the microenvironment polarity with faint fluorescent intensity (low QYs <2%); however, after binding to Aβ_{1-42} aggregates, these probes were efficiently turned on with a significant increase in fluorescent intensity, which makes them a new class of fluorescent probes for Aβ detection.

3.4. Binding Affinity. *In vitro* saturation binding assays were performed to quantitatively explore the affinity of **21a−c** and **22a−c** to Aβ_{1-42} aggregates (Figure S4 in the SI). As shown in Table 1, our probes were demonstrated to have a high to moderate affinity (6.05−56.62 nM). Among these probes, **21b**, **22a**, and **22b** displayed high affinities with K_d values of 6.05, 12.19, and 12.96 nM, respectively, whereas **21c** and **22c** with the longest π-conjugated system displayed moderately decreased affinity of 54.54 and 56.62 nM, respectively. In accordance with our previous work, the torsion caused by too long polyacetylene chain would block the access of our probes to Aβ fibrils, which lead to a decreased affinity.[17] In general, most of these probes (**21a**, **21b**, **22a**, and **22b**) displayed a higher affinity than that of DANIR **2c** (K_d = 26.9 nM) but lower than DANIR **3c** (K_d = 1.9 nM).

Accordingly, peptide fragment Aβ_{16-21} (KLVFFA) with high hydrophobicity is widely accepted as the vital segment for the Aβ aggregation process and serves as the main binding site for small-molecule targeting Aβ plaques.[36,40] To further verify the interaction mechanism between our probes and Aβ plaques, **21b** and **22b** were selected to incubate with segment Aβ_{16-21} (KLVFFA), and the result was obtained with NMR spectroscopy. As shown by the ^{1}H NMR spectra in Figure 4, upon

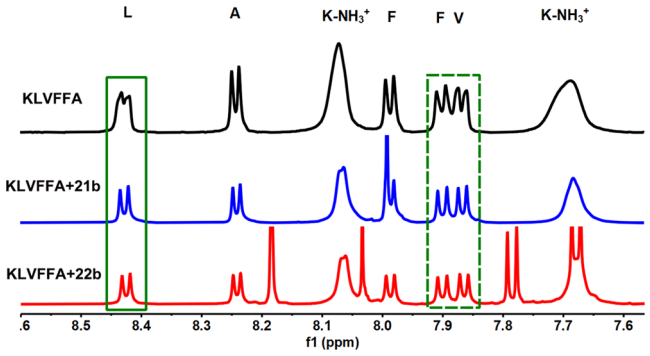

Figure 4. ^{1}H NMR (600 MHz) spectra of KLVFFA alone (black) and upon incubation with **21b** (blue) and **22b** (red). All spectra were recorded in DMSO-d_6 solution at 37 °C. The green boxes indicate the peaks with changes in shape.

incubation with **21b** and **22b**, significant changes in the peak shape of KLVFFA hydrogens were observed: (1) the overlap degree of the F and V hydrogens (indicated by the green dashed box) was decreased and (2) the broad peak of leucine hydrogen (indicated by the green solid box) transformed into a spike, which indicated the interaction between our probes (**21b** and **22b**) and the Aβ_{16-21} segment.

3.5. In Vitro Fluorescent Staining. To explore the feasibility of our probes in the detection of Aβ plaques, *in vitro* fluorescent staining was performed in brain slices from a transgenic (Tg) mouse (APPswe/PSEN1, 13 months old, male) and an AD patient (95 years old, female). As shown in Figures 5

https://dx.doi.org/10.1021/acs.jpcb.0c08845
J. Phys. Chem. B 2021, 125, 497−506

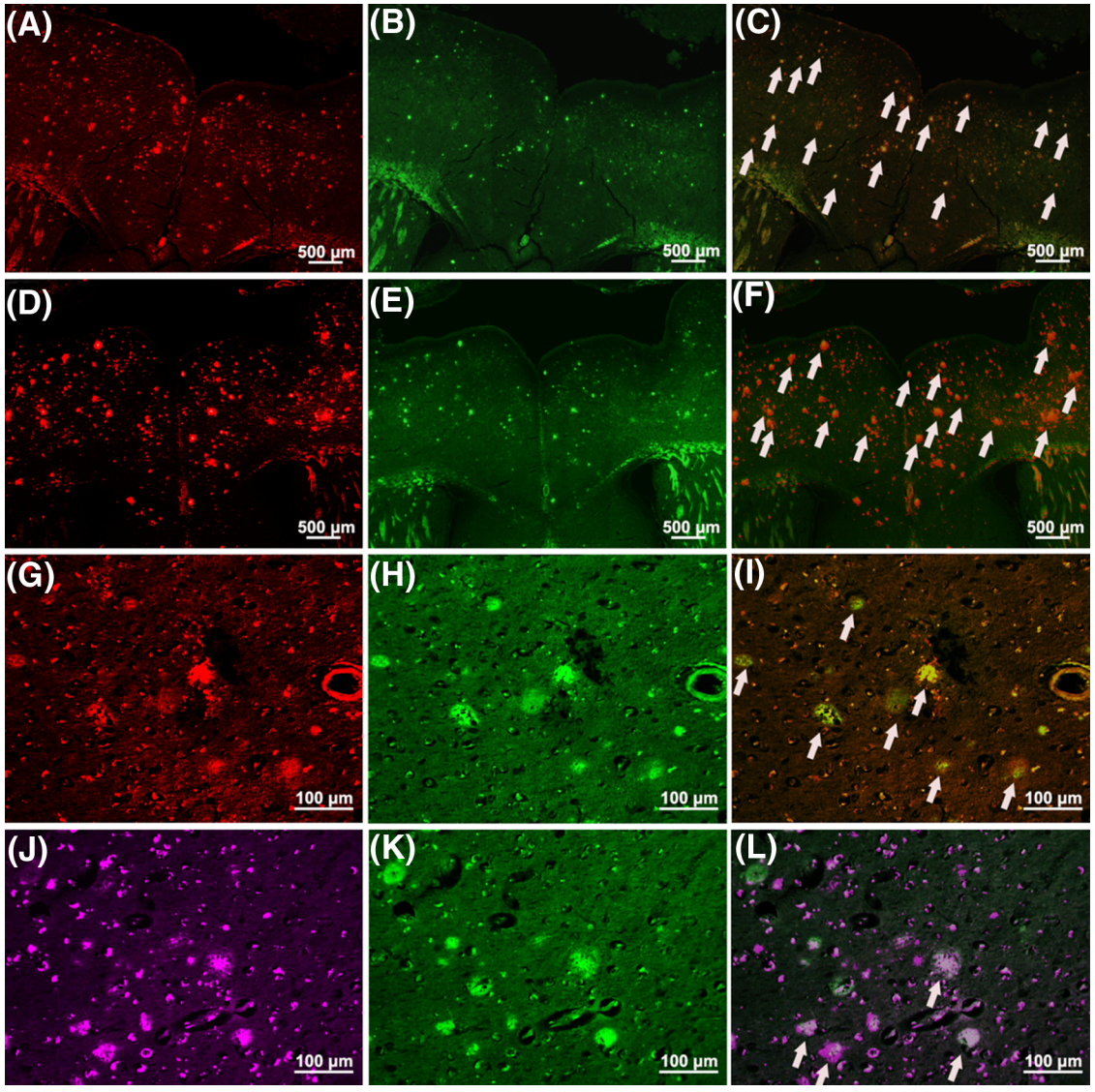

Figure 5. Histological fluorescent staining results in brain sections of Tg mouse (A−F; APPswe/PSEN1, 13 months old, male; magnification, 5×) and AD patients (G−L; 64 years old, female; magnification, 20×) with **21b** (A, G) and **22b** (D, J). These staining results were confirmed by Th-S (middle; B, E, H, K); merge images of the double fluorescent staining results (right: C, F, I, L); and merged senile plaques were indicated by white arrows.

and S5−S7 in the SI, probes **21a**, **21b**, **22a**, and **22b**, which have a higher affinity (<20 nM) and intense fluorescent response toward $A\beta_{1-42}$ aggregates, could precisely identify $A\beta$ plaques in brain slices from both the Tg mouse and AD patient, and these fluorescent patterns were consistent with the staining results of thioflavin-S (Th-S, a traditional fluorescent dye for $A\beta$ plaques). However, **21c** and **22c** with moderate affinities (K_d = 51.54 and 56.62 nM, respectively) displayed undesirable staining patterns: **21c** only showed poor staining performance and **22c** failed to identify any plaques in human brain slices.

4. CONCLUSIONS

In this report, six new D−π−A probes with polyacetylene chains of various lengths were designed, synthesized, and evaluated for the first time as fluorescent probes for $A\beta$ plaques in the brain. Compared with the probes with polyene chains, our new probes displayed irregular emission wavelengths that were not increased with the extension of the π-conjugated system. Furthermore, the QYs of these probes were insensitive to the solvent polarity. Upon interaction with $A\beta_{1-42}$ aggregates, these probes showed a moderate to high affinity and could be turned on with a significant increase in fluorescence intensity (45- to 360-fold). The *in vitro* fluorescent staining results revealed that our probes with high affinity (**21a**, **21b**, **22a**, and **22b**) could efficiently label the $A\beta$ plaques in brain sections from both Tg mouse and AD patient. Of note, compound **22b** with a high affinity (K_d = 12.96 nM) showed remarkable fluorescent responses to $A\beta_{1-42}$ aggregates with an emission maximum at 650 nm, which suggests its potential application in *in vivo* imaging. In summary, we designed and synthesized a series of new $A\beta$ probes that contain polyacetylene chains as a π-conjugated system and successfully used them for *in vitro* detection of $A\beta$ plaques. Our research provides new guidelines for developing smarter and more activatable NIR probes that target $A\beta$.

■ ASSOCIATED CONTENT

Supporting Information

The Supporting Information is available free of charge at https://pubs.acs.org/doi/10.1021/acs.jpcb.0c08845.

https://dx.doi.org/10.1021/acs.jpcb.0c08845
J. Phys. Chem. B 2021, 125, 497−506

Experimental methods; purity determination; optical spectra; binding inhibition studies; *in vitro* fluorescent staining; and ^{1}H NMR, ^{13}C NMR, and HRMS spectra (PDF)

AUTHOR INFORMATION

Corresponding Authors

Hualong Fu − *Key Laboratory of Radiopharmaceuticals, Ministry of Education, College of Chemistry, Beijing Normal University, Beijing 100875, China*; Phone: +86-18701178045; Email: fuhualong@bnu.edu.cn

Mengchao Cui − *Key Laboratory of Radiopharmaceuticals, Ministry of Education, College of Chemistry, Beijing Normal University, Beijing 100875, China*; orcid.org/0000-0002-3488-7864; Phone: +86-13811995064; Email: cmc@bnu.edu.cn

Authors

Longfei Zhang − *Key Laboratory of Radiopharmaceuticals, Ministry of Education, College of Chemistry, Beijing Normal University, Beijing 100875, China*

Xin Gong − *Key Laboratory of Radiopharmaceuticals, Ministry of Education, College of Chemistry, Beijing Normal University, Beijing 100875, China*

Chuan Tian − *Key Laboratory of Radiopharmaceuticals, Ministry of Education, College of Chemistry, Beijing Normal University, Beijing 100875, China*

Hongwei Tan − *Key Laboratory of Radiopharmaceuticals, Ministry of Education, College of Chemistry, Beijing Normal University, Beijing 100875, China*

Jiapei Dai − *Wuhan Institute for Neuroscience and Neuroengineering, South-Central University for Nationalities, Wuhan 430074, China*; orcid.org/0000-0002-1474-5754

Complete contact information is available at: https://pubs.acs.org/10.1021/acs.jpcb.0c08845

Author Contributions

M.C., H.F., and L.Z. conceived and designed the experiment. L.Z. and C.T. synthesized and characterized final probes. Optical properties were determined by L.Z. *In vitro* saturation binding assays were performed by L.Z. *In vitro* fluorescent staining was performed by L.Z. M.C. and J.D. contributed reagents, materials, and analysis tools. M.C., H.F., and L.Z. wrote the paper.

Notes

The authors declare no competing financial interest.

ACKNOWLEDGMENTS

This work was supported by the National Natural Science Foundation of China (nos. U1967221 and 22022601)

ABBREVIATIONS USED

AD, Alzheimer's disease; Aβ, β-amyloid; BSA, bovine serum albumin; DCM, dichloromethane; DMP, Dess−Martin periodinane reagent; DMSO, dimethyl sulfoxide; Et_3N, triethylamine; LUMO, lowest unoccupied molecular orbital; HOMO, highest occupied molecular orbital; HPLC, high-performance liquid chromatography; HRMS, high-resolution mass spectrometry; ICT, intramolecular charge transfer; MS, mass spectrometry; NIR, near-infrared; NMR, nuclear magnetic resonance; PBS, phosphate-buffered saline; QY, quantum yield; rt, room temperature; SI, Supporting Information; TBAF, tetrabutylammonium fluoride; Tg, transgenic; THF, tetrahydrofuran; Th-S, thioflavin-S; TLC, thin-layer chromatography; TMEDA, tetramethylethylenediamine

REFERENCES

(1) Brookmeyer, R.; Johnson, E.; Ziegler-Graham, K.; Arrighi, H. M. Forecasting the Global Burden of Alzheimer's Disease. *Alzheimer's Dementia* **2007**, *3*, 186−191.

(2) Small, G. Early Diagnosis of Alzheimer's Disease. *New Dir. Ment. Health Serv.* **1997**, *24*, 39−51.

(3) Ariza, M.; Kolb, H. C.; Moechars, D.; Rombouts, F.; Andres, J. I. Tau Positron Emission Tomography (PET) Imaging: Past, Present, and Future. *J. Med. Chem.* **2015**, *58*, 4365−4382.

(4) Yang, P.; Perlmutter, J. S.; Benzinger, T. L. S.; Morris, J. C.; Xu, J. Dopamine D3 Receptor: A Neglected Participant in Parkinson Disease Pathogenesis and Treatment? *Ageing Res. Rev.* **2020**, *57*, No. 100994.

(5) Hardy, J.; Selkoe, D. J. The Amyloid Hypothesis of Alzheimer's Disease: Progress and Problems on the Road to Therapeutics. *Science* **2002**, *297*, 353−356.

(6) Cui, M. Past and Recent Progress of Molecular Imaging Probes for Beta-Amyloid Plaques in the Brain. *Curr. Med. Chem.* **2013**, *21*, 82−112.

(7) Hardy, J. The shorter amyloid cascade hypothesis. *Neurobiol. Aging* **1999**, *20*, 85.

(8) Weiner, H. L.; Frenkel, D. Immunology and Immunotherapy of Alzheimer's Disease. *Nat. Rev. Immunol.* **2006**, *6*, 404−416.

(9) Nitsch, R. M.; Hock, C. Targeting Beta-Amyloid Pathology in Alzheimer's Disease with Abeta Immunotherapy. *Neurotherapeutics* **2008**, *5*, 415−420.

(10) James, M. L.; Gambhir, S. S. A Molecular Imaging Primer: Modalities, Imaging Agents, and Applications. *Physiol. Rev.* **2012**, *92*, 897−965.

(11) Cui, M.; Ono, M.; Watanabe, H.; Kimura, H.; Liu, B.; Saji, H. Smart Near-Infrared Fluorescence Probes with Donor-Acceptor Structure for in vivo Detection of Beta-amyloid Deposits. *J. Am. Chem. Soc.* **2014**, *136*, 3388−3394.

(12) Licha, K.; Olbrich, C. Optical Imaging in Drug Discovery and Diagnostic Applications. *Adv. Drug Delivery Rev.* **2005**, *57*, 1087−1108.

(13) Ji, Y.; Jones, C.; Baek, Y.; Park, G. K.; Kashiwagi, S.; Choi, H. S. Near-Infrared Fluorescence Imaging in Immunotherapy. *Adv. Drug Delivery Rev.* **2020**, *167*, 121−134.

(14) Gyasi, Y. I.; Pang, Y. P.; Li, X. R.; Gu, J. X.; Cheng, X. J.; Liu, J.; Xu, T.; Liu, Y. Biological Applications of Near Infrared Fluorescence Dye Probes in Monitoring Alzheimer's Disease. *Eur. J. Med. Chem.* **2020**, *187*, No. 111982.

(15) Aliyan, A.; Cook, N. P.; Marti, A. A. Interrogating Amyloid Aggregates Using Fluorescent Probes. *Chem. Rev.* **2019**, *119*, 11819−11856.

(16) Owens, E. A.; Henary, M.; El Fakhri, G.; Choi, H. S. Tissue-Specific Near-Infrared Fluorescence Imaging. *Acc. Chem. Res.* **2016**, *49*, 1731−1740.

(17) Fu, H.; Cui, M.; Zhao, L.; Tu, P.; Zhou, K.; Dai, J.; Liu, B. Highly Sensitive Near-Infrared Fluorophores for in Vivo Detection of Amyloid-Beta Plaques in Alzheimer's Disease. *J. Med. Chem.* **2015**, *58*, 6972−6983.

(18) Qian, G.; Zhong, Z.; Luo, M.; Yu, D.; Zhang, Z.; Wang, Z. Y.; Ma, D. Simple and Efficient Near-Infrared Organic Chromophores for Light-Emitting Diodes with Single Electroluminescent Emission above 1000 nm. *Adv. Mater.* **2009**, *21*, 111−116.

(19) Bricks, J. L.; Kachkovskii, A. D.; Slominskii, Y. L.; Gerasov, A. O.; Popov, S. V. Molecular Design of Near Infrared Polymethine Dyes: A Review. *Dyes Pigm.* **2015**, *121*, 238−255.

(20) Tatikolov, A. S. Polymethine Dyes as Spectral-Fluorescent Probes for Biomacromolecules. *J. Photochem. Photobiol., C* **2012**, *13*, 55−90.

(21) Zhou, K.; Bai, H.; Feng, L.; Dai, J.; Cui, M. Smart D-pi-A Type Near-Infrared Abeta Probes: Effects of A Marked Pi Bridge on Optical and Biological Properties. *Anal. Chem.* **2017**, *89*, 9432−9437.

(22) Fu, H.; Tu, P.; Zhao, L.; Dai, J.; Liu, B.; Cui, M. Amyloid-Beta Deposits Target Efficient Near-Infrared Fluorescent Probes: Synthesis,

in Vitro Evaluation, and in Vivo Imaging. *Anal. Chem.* **2016**, *88*, 1944−1950.
(23) Liu, J.; Lam, J. W.; Tang, B. Z. Acetylenic Polymers: Syntheses, Structures, and Functions. *Chem. Rev.* **2009**, *109*, 5799−5867.
(24) Haque, A.; Al-Balushi, R. A.; Al-Busaidi, I. J.; Khan, M. S.; Raithby, P. R. Rise of Conjugated Poly-ynes and Poly(Metalla-ynes): From Design Through Synthesis to Structure-Property Relationships and Applications. *Chem. Rev.* **2018**, *118*, 8474−8597.
(25) Bunz, U. H. Poly(aryleneethynylene)s. *Macromol. Rapid Commun.* **2009**, *30*, 772−805.
(26) Donabedian, P. L.; Pham, T. K.; Whitten, D. G.; Chi, E. Y. Oligo(p-phenylene ethynylene) Electrolytes: A Novel Molecular Scaffold for Optical Tracking of Amyloids. *ACS Chem. Neurosci.* **2015**, *6*, 1526−1535.
(27) Donabedian, P. L.; Creyer, M. N.; Monge, F. A.; Schanze, K. S.; Chi, E. Y.; Whitten, D. G. Detergent-Induced Self-Assembly and Controllable Photosensitizer Activity of Diester Phenylene Ethynylenes. *Proc. Natl. Acad. Sci. U.S.A.* **2017**, *114*, 7278−7282.
(28) Frank, B. B.; Laporta, P. R.; Breiten, B.; Kuzyk, M. C.; Jarowski, P. D.; Schweizer, W. B.; Seiler, P.; Biaggio, I.; Boudon, C.; Gisselbrecht, J.-P.; Diederich, F. Comparison of CC Triple and Double Bonds as Spacers in Push-Pull Chromophores. *Eur. J. of Org. Chem.* **2011**, *2011*, 4307−4317.
(29) Li, Y.; Wang, K.; Zhou, K.; Guo, W.; Dai, B.; Liang, Y.; Dai, J.; Cui, M. Novel D-A-D Based Near-Infrared Probes for the Detection of Beta-Amyloid and Tau Fibrils in Alzheimer's Disease. *Chem. Commun.* **2018**, *54*, 8717−8720.
(30) Fu, Z.; Hao, G.; Fu, Y.; He, D.; Tuo, X.; Guo, S.; Cai, H. Transition Metal-Free Electrocatalytic Halodeborylation of Arylboronic Acids with Metal Halides MX (X = I, Br) to Synthesize Aryl Halides. *Org. Chem. Front.* **2020**, *7*, 590−595.
(31) Sharber, S. A.; Shih, K. C.; Mann, A.; Frausto, F.; Haas, T. E.; Nieh, M. P.; Thomas, S. W. Reversible Mechanofluorochromism of Aniline-Terminated Phenylene Ethynylenes. *Chem. Sci.* **2018**, *9*, 5415−5426.
(32) Hrobarikova, V.; Hrobarik, P.; Gajdos, P.; Fitilis, I.; Fakis, M.; Persephonis, P.; Zahradnik, P. Benzothiazole-Based Fluorophores of Donor-Pi-Acceptor-Pi-Donor Type Displaying High Two-Photon Absorption. *J. Org. Chem.* **2010**, *75*, 3053−3068.
(33) Moussaoui, Y.; Ben Salem, R. Catalyzed Knoevenagel Reactions on Inorganic Solid Supports: Application to the Synthesis of Coumarine Compounds. *C. R. Chim.* **2007**, *10*, 1162−1169.
(34) Fleming, C. L.; Sandoz, P. A.; Inghardt, T.; Onfelt, B.; Grotli, M.; Andreasson, J. A Fluorescent Kinase Inhibitor that Exhibits Diagnostic Changes in Emission upon Binding. *Angew. Chem., Int. Ed.* **2019**, *58*, 15000−15004.
(35) Zhang, X.; Tian, Y.; Li, Z.; Tian, X.; Sun, H.; Liu, H.; Moore, A.; Ran, C. Design and Synthesis of Curcumin Analogues for in Vivo Fluorescence Imaging and Inhibiting Copper-Induced Cross-Linking of Amyloid Beta Species in Alzheimer's Disease. *J. Am. Chem. Soc.* **2013**, *135*, 16397−16409.
(36) Rzepecki, P.; Schrader, T. Beta-Sheet Ligands in Action: KLVFF Recognition by Aminopyrazole Hybrid Receptors in Water. *J. Am. Chem. Soc.* **2005**, *127*, 3016−3025.
(37) Staderini, M.; Martin, M. A.; Bolognesi, M. L.; Menendez, J. C. Imaging of Beta-Amyloid Plaques by Near Infrared Fluorescent Tracers: A New Frontier for Chemical Neuroscience. *Chem. Soc. Rev.* **2015**, *44*, 1807−1819.
(38) Yao, L.; Zhang, S.; Wang, R.; Li, W.; Shen, F.; Yang, B.; Ma, Y. Highly Efficient Near-Infrared Organic Light-Emitting Diode Based on A Butterfly-Shaped Donor-Acceptor Chromophore with Strong Solid-State Fluorescence and A Large Proportion of Radiative Excitons. *Angew. Chem., Int. Ed.* **2014**, *53*, 2119−2123.
(39) Blanchard-Desce, M.; Wortmann, R.; Lebus, S.; Lehn, J.-M.; Krämer, P. Intramolecular Charge Transfer in Elongated Donor-Acceptor Conjugated Polyenes. *Chem. Phys. Lett.* **1995**, *243*, 526−532.
(40) Zhou, K.; Yuan, C.; Dai, B.; Wang, K.; Chen, Y.; Ma, D.; Dai, J.; Liang, Y.; Tan, H.; Cui, M. Environment-Sensitive Near-Infrared Probe for Fluorescent Discrimination of Abeta and Tau Fibrils in AD Brain. *J. Med. Chem.* **2019**, *62*, 6694−6704.

https://dx.doi.org/10.1021/acs.jpcb.0c08845
J. Phys. Chem. B 2021, 125, 497−506